Data reduction strategies at a time-of-flight NSE for a lamellar microemulsion

Olaf Holderer[1,*], *Henrich* Frielinghaus[1], *Piotr* Zolnierczuk[2], *Michael* Ohl[3], and *Michael* Monkenbusch[3]

[1]1Jülich Centre for Neutron Science (JCNS) at Heinz Maier-Leibnitz Zentrum (MLZ), Forschungszentrum Jülich GmbH, Garching, Germany
[2]SNS - Oak Ridge National Laboratory, Oak Ridge, TN, USA
[3]Jülich Centre for Neutron Science (JCNS), Forschungszentrum Jülich GmbH, Jülich, Germany

Abstract. Neutron spin echo (NSE) spectroscopy provides the ultimate energy resolution in quasi-elastic thermal and cold neutron scattering spectroscopy. A peculiarity of the SNS-NSE, the only NSE spectrometer at a pulsed beam port at the moment, is that the wavelength spread $\delta\lambda/\lambda$ can be chosen during evaluation with an appropriate time channel binning. The Q-resolution can be adjusted in certain limits a posteriori by choosing the appropriate detector binning (as on a continuous source) and time channel binning. This can be exploited for samples with a strongly varying scattering function $S(Q,t)$, e.g. due to Bragg peaks in a crystal or lamellar ordering in microemulsions. The data reduction software DrSpine allows for appropriate slicing and masking for this task. In this contribution the correlation function of microemulsions, thermodynamically stable mixtures of oil, water and surfactant, is measured with NSE on length scales where structural correlations are important, and data reduction strategies varying the Q-resolution by pixel and time channel grouping are discussed. The typical "de Gennes narrowing" or structural narrowing is observed with a relaxation time proportional to $I(Q)$. In these regions of strongly varying intensity it is shown that a too coarse grouping has an influence on the data reduction, with a broadened in Q of the apparent slowing down.

1 Introduction

Microemulsions, i.e. thermodynamically stable mixtures of water, oil and a surfactant, can form different structures such as bicontinuous, lamellar or droplet structures. Neutron scattering is a well suited tool for studying soft matter in terms of its structural and dynamic properties. The bending elasticity or rigidity of microemulsions can be studied with neutron spin-echo spectroscopy (NSE), the highest resolution spectroscopic technique in neutron scattering [1]. The intermediate scattering function determined with NSE pertains to the Fourier transform of the height correlation function and follows approximately a stretched exponential decay for large scattering vectors Q [2]. The influence of the correlation peak on the dynamics has been studied with NSE spectroscopy by looking at bulk bicontinuous microemulsions, but without preferrential ordering, in Ref. [3] and interpreted in terms of hydrodynamic effects [4]. Lamellar microemulsions have been studied with NSE by Mihailescu et al.[5] in detail with added diblock copolymers as an emulsification booster. A single crystal of a lyotropic L_α-phase has been investigated with neutron diffraction by Göcking et al. [6]. A similar oriented lamellar phase has been studied with small angle scattering in order to shed light on electrostatic and steric interactions in such phases [7]. The dynamics of lipid membrane stacks has been studied with NSE in order to observe different fluctuation modes [8, 9], using stacks of lipid bilayers. This allows for a precise measurement of the scattering vector in different directions, in plane and out of plane. Similarly, measurements under grazing incidence conditions allows for a very precise sample geometry for studying microemulsions or lipid membranes [10, 11]. Also neutron reflectometry gives some insight in the structure and dynamics of lamellar stacks by the analysis of the scattering peak shape [12]

Here we want to demonstrate how the time-of-flight mode of a neutron spin echo spectrometer at a spallation source affects the planning and data evaluation of such experiments on structured samples. A more detailed analysis of the deduced bending constants and structural properties of these types of microemulsions can be found e.g. in Refs. [5, 13, 14].

2 Experimental

2.1 Samples

Lamellar microemulsions were prepared with deuterated decane, D_2O and the surfactant $C_{10}E_4$. At surfactant concentrations of Ψ = 21 vol% a lamellar phase is formed in such systems [15]. To align the microemulsion in the beam, a cell with quartz lamellae has been used, where the microemulsion is sheared into the gap of 0.2 mm between two lamellae. The lamellae are stacked to fill the full beam. The same cells and samples have been used also in Ref. [16]. The bicontinuous microemulsion which serves as a comparison was prepared with Ψ = 17 vol%. Details of the used materials and the bulk microemulsion can be found in Ref. [17].

*e-mail: o.holderer@fz-juelich.de

2.2 Neutron Spin Echo Spectroscopy

Experiments have been carried out at the SNS-NSE at the Oak Ridge National Laboratory [18]. Due to the pulsed neutron source the wavelength of each detected neutron can be tagged by the moderator to detector time-of-flight (TOF). The experiments have been carried out with a wavelength band of 6-9 Å and two scattering angles, for the lamellar sample corresponding to $Q_{center,lam-min}$ = 0.065 Å^{-1} and 0.08 Å^{-1}, covering a Q-range from 0.04-0.15 Å^{-1}. The bicontinuous microemulsion with different structural parameters has been measured at $Q_{center,lam-min}$ = 0.11 Å^{-1} and 0.14 Å^{-1}.

3 Results and Discussion

The microemulsion in the lamellar cell is in an oriented lamellar phase at a temperature of 301 K. The sample cell temperature was set with a copper frame connected to a water thermostat. Aluminum sheets acted as a heat shield in the beam window area. The set point of the thermostat was 305 K allowing for an temperature offset induced by the air conditioning in the SNS-NSE cave. The lower phase boundary to the bicontinuous phase is approximately at 298-299 K.

The inherent time-of-flight mode of the SNS-NSE allows to adjust the wavelength spread during data evaluation by choosing the desired binning over the detector and across the 42 time channels which cover the wavelength band of 3 Å width. Since the sample shows a significant structuring in the Q-range of this experiment with strong correlation peaks, the 32x32 pixel detector was evaluated with different binnings of the detector pixels and time channels. The finest evaluation used the 32x32 detector pixelwise, and the time channels have been grouped into 9 slices. Different detector and time binnings have been tried out and are also presented in the following discussion. Data reduction has been done with the DrSpine software [19]. For the lamellar phase, a detector mask has been applied which covers only a stripe in the middle of the detector, i.e. around $Q_y = 0$. Figure 1 shows the corresponding mask for the full 32x32 pixel detector. Regions marked with 1 are excluded from the evaluation. For other binning during evaluation, the mask has been adapted to cover the same stripe as in Figure 1. A typical detector image of one time bin is shown in Figure 2. The stripe along the x-direction is used for the data treatment of the lamellar phase and corresponds to the region not masked as shown in Figure 1.

The intermediate scattering function for bicontinuous and lamellar phase are shown in Fig. 3. The strong scattering intensity allows for a detailed evaluation of the bicontinuous microemulsion over the whole Q-range measured in this experiment. Since the lamellar phase is strongly structured, the statistics worsens due to the low count rate away from the structure factor peak maximum. The histogrammed intensity as a function of Q as shown in Fig. 4 exhibits for the lamellar phase a correlation peak at Q≃ 0.07 Å^{-1} corresponding to the average distance between surfactant layers, and the second order peak at Q≃ 0.14 Å^{-1}. The corresponding length scale $d_{surf} = 2\pi/q$

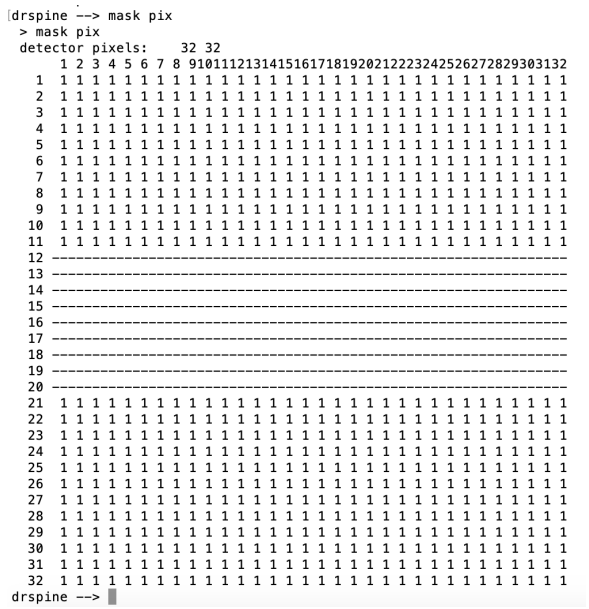

Figure 1. Detector mask applied for the lamellar phase. All pixels marked with 1 are excluded from the evaluation. In this representation the main direction of Q-variation is horizontal.

is 90 Å. The domain size of a bicontinuous microemulsion d=37 Å / Ψ would result in d_{domain}=176 Å and d_{surf} = $d_{domain}/2$ = 88 Å. This indicates that the temperature at the sample might be slightly outside the purely lamellar temperature window with more disorder leading to a larger average distance between lamellae. A perfectly flat lamellar phase would have d=24 Å / Ψ = 114 Å for d_{domain} or 57 Å for d_{surf}. In Figure 4 an attempt has been made for an absolute scaling of the two samples by normalizing the raw scattering data from the SNS-NSE with an absolute measurement of I(Q) vs Q of a bicontinuous microemulsion with similar surfactant contents from a SANS experiment [14]. The histogram of the bicontinuous phase has been fitted with a polynomial of degree 5, the ratio between this fit and the fitted I(Q) of the absolute SANS experiment provides the correction factor for this experiment. The corrected intensity in Figure 4 represents roughly the SANS intensity on an absolute scale.

Both, the bicontinuous microemulsion and the lamellar microemulsion have been fitted with the amplitude left free, since in microemulsion measurements a proper background subtraction is difficult since the proper oil/water solvent without surfactant can not be prepared. In regions of low intensity (away from the structure factor peak in the lamellar phase or at high Q in the bicontinuous phase), the missing background subtraction requires the amplitude as a fitting parameter. The comparison between the relaxation time τ_0(Q) and the intensity I(Q) is illustrated by figures 4 and 5, both as a function of Q. It shows that $\tau_0(Q) \propto$ I(Q) for the lamellar microemulsion, whereas the bicontinuous microemulsion shows a strong reduction of the relaxation time proportional to Q^{-3} as expected from the height fluctuation model from Zilman and Granek [2]. It has to be pointed out that the relaxation time at the peak position

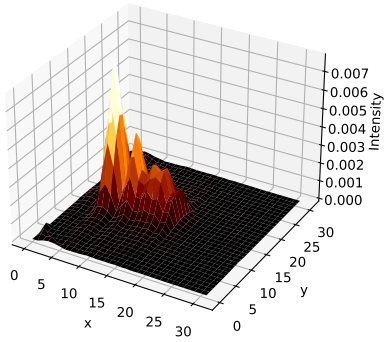

Figure 2. Average intensity at the detector for the oriented lamellar microemulsion with the strong correlation peak. Directions are $x \rightarrow Q_z$ and $y \rightarrow Q_{\text{parallel}}$. The subpeak type modulation is an artifact induced by the analyzer mirror stacking.

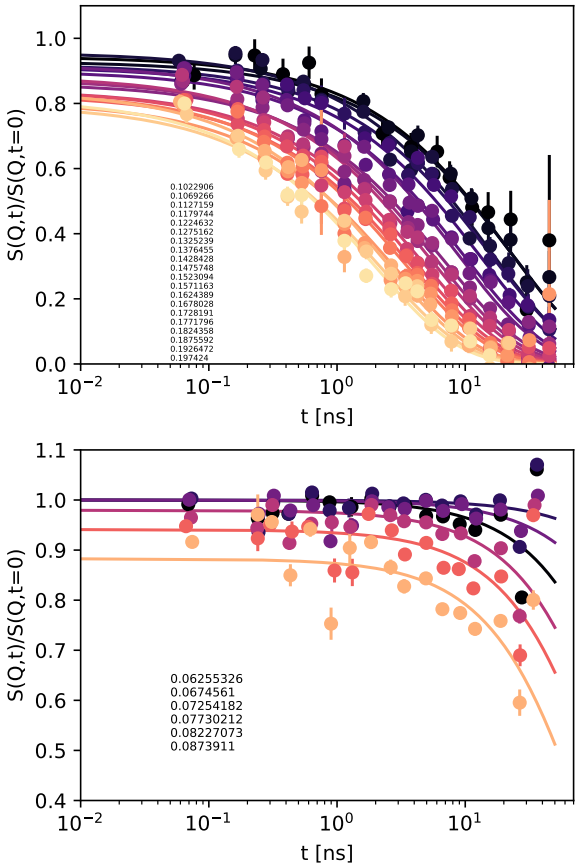

Figure 3. Intermediate scattering function S(q,t)/S(q,0) for a bicontinuous (top) and an oriented lamellar microemulsion (bottom).

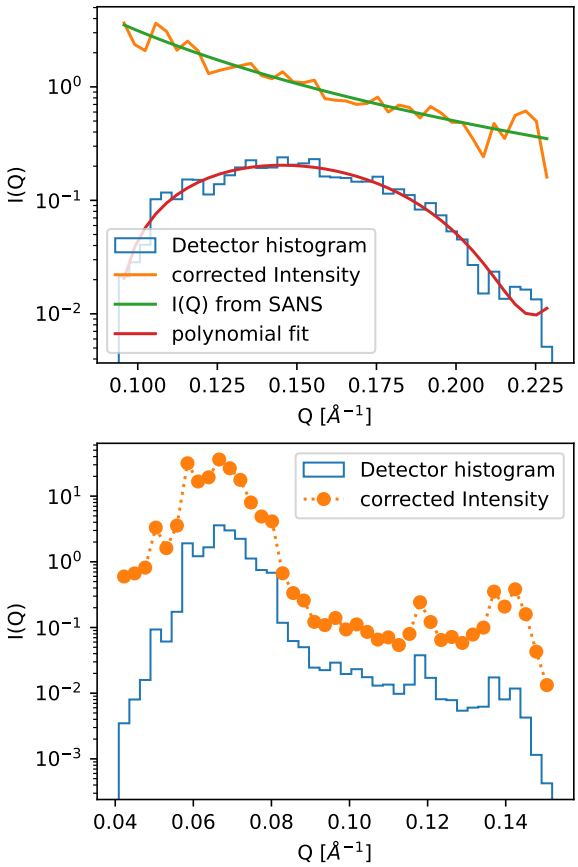

Figure 4. Histogram of q-intensities of the NSE experiment for the bicontinuous (top) and lamellar microemulsion (bottom). From previous SANS experiments on bicontinuous microemulsions the relevant Q-range has been fitted on an absolute scale and used to determine the detector sensitivity.

can not be resolved any more in the current time range of the experiment and represents a basically elastic situation without relaxation in the observation time window. Figure 6 illustrates the effective diffusion coefficient $D = 1/(\tau_0 Q^2)$ with a roughly linear increase for the bicontinuous phase (as expected for the Q^{-3}-dependence) and the strong slowing down in the lamellar phase at the q-position of the correlation peak. The low scattering intensity off the peak position results in a strong scattering of the data above Q=0.1 Å^{-1}. For a more detailed analysis of the bicontinuous phase we refer to fits with the full Zilman-Granek model to such microemulsion systems in Refs [10, 14].

The wavelength band used at the SNS-NSE has a width of 3 Åsplit into 42 time channels for a single pulse. The ΔQ of a time channel is approximately 0.0012-0.0005 Å^{-1} (for the wavelength band of 6-9 Å), the Q-width of a single detector pixel of the 32x32 pixel detector is 0.0026-0.0017 Å^{-1} for the same wavelength band (as inferred from the nse scan). An adequate combination of timechannel binning and detector binning would be 2 time channels for the pixel wise evaluation, 5 time channels for a 2x2 pixel grouping and 10 time channels for the 4x4 pixel grouping evaluation (of the 32x32 pixel detector, where the mask of Fig 1 has been applied). The variation of Q may differ

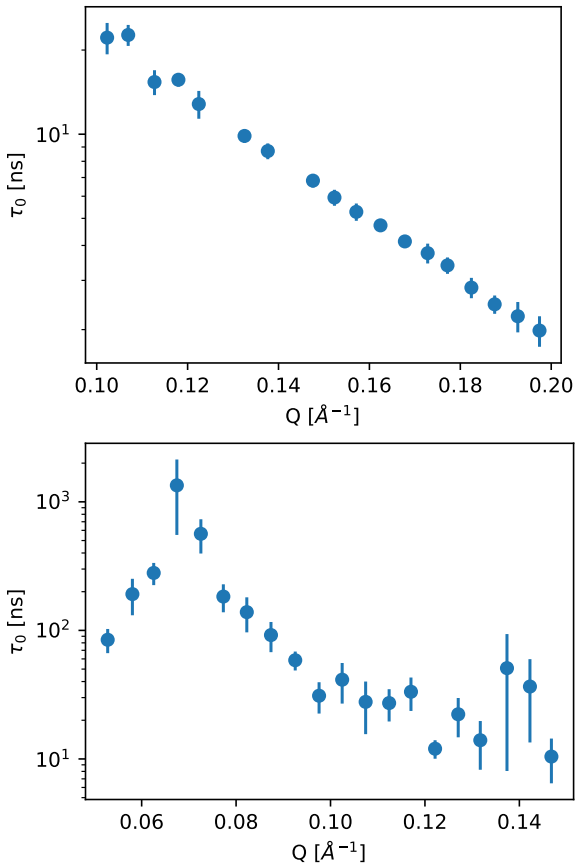

Figure 5. Relaxation time as function of scattering vector for the bicontinuous microemulsion (top) and the ordered lamellar microemulsion (bottom).

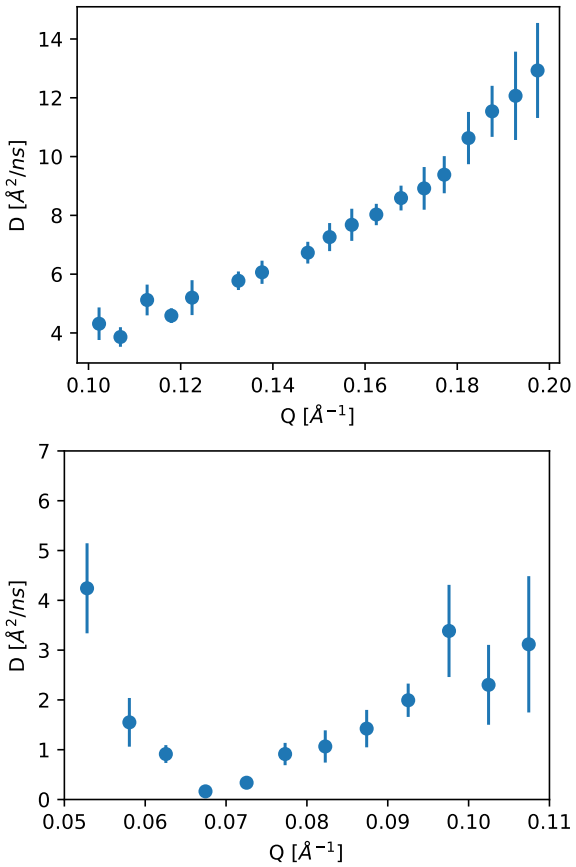

Figure 6. Diffusion constant (i.e. $1/(\tau_0 Q^2)$ for the bicontinuous (top) and lamellar (bottom) microemulsion.

from the minimal possible variation and is determined by the histogramming procedure in the evaluation.

The evaluation has been run in the Q-range of 0.05-0.15 Å^{-1}, with 20, 10 and 5 Q-bins i.e. with a distance between Q's of 0.005 Å^{-1}, 0.01 Å^{-1} and 0.02 Å^{-1}. The Q-variation within the final Q-bins was always about one order of magnitude better than the Q-steps. The limiting factor is therefore not the instrumental capabilities in terms of Q-resolution, but the statistics of the experiment.

The major limiting factor of the Q resolution of the NSE instrument is the beam divergence. It is determined by the size of the neutron guide exit (40 mm x 60 mm), the sample size (30 mm x 30 mm) and the distance between neutron guide and sample (approx. 4 m), leading to about ±0.5° beam divergence. This translates to a ΔQ due to the angular divergence between 0.012 and 0.018 Å^{-1} depending on the wavelength.

The choice of a grouping of 4x4 pixels on the detector matches this divergence quite well.

On the other hand, the lamellar phase acts as a monochromator and affects to some extend the divergence after the scattering process. Especially around the peak position, a fine evaluation has an advantage, also because the intensity variation across the pixel is smaller and better comparable between reference and sample. Figure 7 shows the effect of different binnings and Q collection steps. Around the peak position the statistics is good enough for a single pixel evaluation. Grouping 2x2 pixels together works similarly well. The coarser grouping of 4x4 pixels for the evaluation shows some deviations in the diffusion constant around the peak, although this would be the best matching conditions. Beyond approximately Q=0.1 Å^{-1} the errorbars get too large to compare the different evaluation schemes, it has therefore been omitted. The strong intensity at the peak position dominates the 4x4 grouping evaluation even for pixels centered a bit aside of the peak. Therefore the very slow peak relaxation influences also Q's aside of the peak, if the groupig is coarser.

Omitting the stripe mask for the lamellar phase results in a stronger variation of the resulting relaxation times and diffusion constants due to the added noise of the detector regions with low count rate.

4 Conclusion

The membrane dynamics of a lamellar microemulsion has been studied with the time-of-flight NSE spectrometer, where the Q-resolution can be adjusted by appropriate binning during the data reduction. The structural slowing down has been observed also in this lamellar microemulsion. At Q-values directly beyond the first correlation peak the linear increase of the diffusion constant calculated from the relaxation time shows the height fluctuation signature with a Q^3 dependence of the relaxation rate.

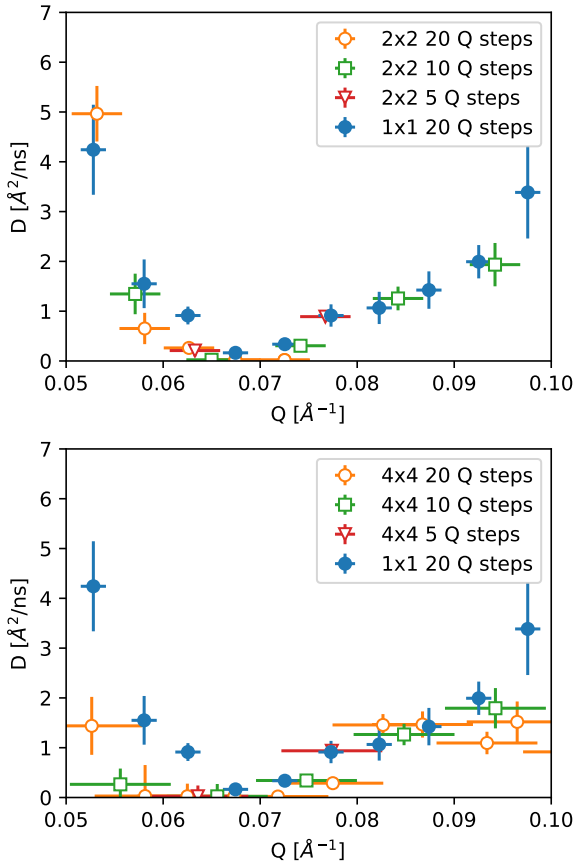

Figure 7. Variation of pixel binning and Q-binning: the most significant difference is the lower diffusion constant if evaluated with a coarser binning, most likely due to contributions from the Bragg peak contributing to more Q-bins. The 2x2 pixel grouping evaluation seems to be a good compromise between statistics and resolution. The dQ errorbars represent the error in Q due to the pixel grouping only.

The Q-resolution provided by the SNS-NSE instrument is mainly governed by the beam divergence in the current experiment. Reducing the pixel binning by grouping 2x2 pixels or using single pixels seems to be advantageous over a too coarse binning. This might be due to subtle resolution effects due to the scattering at the oriented lamellar membrane stack. Only very close to the correlation peak the obtained relaxation time (or diffusion constant) was slightly modified by this effect. The high intensity and slow relaxation at the peak position influences also pixel groups aside of the peak, the more the larger the evaluation pixels are chosen. The limitation is still the intensity per pixel, which prevents a single pixel, single (or two) time channel binning for nominal highest resolution. When conducting such experiments with the presence of correlation peaks on the detector, it has to be taken into account that smaller binnings during evaluation are required, and also that the intensity might vary strongly between the peak region and further away from the peak. The counting time has to be adapted accordingly. These effects of structure factor peaks in the Q-region of the experiment are important not only in such lamellar or structured systems where the dynamics of the system itself is slowed down by the structure factor influence, but also in confined or multi-component materials, where an elastic signal from the matrix might be avoided by chosing the relevant Q-binning. If even sharper Q-resolution is required, then also smaller samples and entrance slits have to be used. Another example might be experiments with large fluctuating magnetic structures such as Skyrmions, where sharp magnetic Bragg peaks are surrounded by weak and slow fluctuations, this high Q resolution might be fully exploited.

Data availabilit statement

The data from the NSE experiments are available from the corresponding author upon reasonable request.

Acknowledgement

This research at Oak Ridge National Laboratory's Spallation Neutron Source was sponsored by the Scientific User Facilities Division, Office of Basic Energy Sciences, US Department of Energy.

References

[1] F. Mezei, in *Neutron spin echo* (Springer, 1980), pp. 1–26
[2] A. Zilman, R. Granek, Physical review letters **77**, 4788 (1996)
[3] O. Holderer, H. Frielinghaus, M. Monkenbusch, J. Allgaier, D. Richter, B. Farago, The European Physical Journal E **22**, 157 (2007)
[4] M. Nonomura, T. Ohta, The Journal of chemical physics **110**, 7516 (1999)
[5] M. Mihailescu, M. Monkenbusch, J. Allgaier, H. Frielinghaus, D. Richter, B. Jakobs, T. Sottmann, Physical Review E **66**, 041504 (2002)
[6] K. Goecking, M. Monkenbusch, EPL (Europhysics Letters) **43**, 135 (1998)
[7] F. Nallet, D. Roux, S. Milner, Journal de Physique **51**, 2333 (1990)
[8] C.L. Armstrong, W. Häußler, T. Seydel, J. Katsaras, M.C. Rheinstädter, Soft matter **10**, 2600 (2014)
[9] M.C. Rheinstädter, W. Häußler, T. Salditt, Physical review letters **97**, 048103 (2006)
[10] H. Frielinghaus, M. Kerscher, O. Holderer, M. Monkenbusch, D. Richter, Physical Review E **85**, 041408 (2012)
[11] S. Jaksch, O. Holderer, M. Gvaramia, M. Ohl, M. Monkenbusch, H. Frielinghaus, Scientific Reports **7**, 4417 (2017)
[12] T. Salditt, C. Münster, U. Mennicke, C. Ollinger, G. Fragneto, Langmuir **19**, 7703 (2003)
[13] M. Mihailescu, M. Monkenbusch, H. Endo, J. Allgaier, G. Gompper, J. Stellbrink, D. Richter, B. Jakobs, T. Sottmann, B. Farago, The Journal of Chemical Physics **115**, 9563 (2001)
[14] O. Holderer, H. Frielinghaus, D. Byelov, M. Monkenbusch, J. Allgaier, D. Richter, The Journal of chemical physics **122**, 094908 (2005)

[15] D. Byelov, H. Frielinghaus, O. Holderer, J. Allgaier, D. Richter, Langmuir **20**, 10433 (2004)

[16] O. Holderer, H. Frielinghaus, D. Byelov, M. Monkenbusch, D. Richter et al., Zeitschrift für Physikalische Chemie **224**, 243 (2010)

[17] F. Lipfert, O. Holderer, H. Frielinghaus, M.S. Appavou, C. Do, M. Ohl, D. Richter, Nanoscale **7**, 2578 (2015)

[18] M. Ohl, M. Monkenbusch, N. Arend, T. Kozielewski, G. Vehres, C. Tiemann, M. Butzek, H. Soltner, U. Giesen, R. Achten et al., Nuclear Instruments and Methods in Physics Research Section A: Accelerators, Spectrometers, Detectors and Associated Equipment **696**, 85 (2012)

[19] P. Zolnierczuk, O. Holderer, S. Pasini, T. Kozielewski, L. Stingaciu, M. Monkenbusch, Journal of applied crystallography **52** (2019)